Hindawi
Advances in Civil Engineering
Volume 2018, Article ID 9327403, 8 pages
https://doi.org/10.1155/2018/9327403

Research Article

Combined Effect of Vertical and Horizontal Ground Motions on Failure Probability of RC Chimneys

Xuan Guo,[1,2] **Wei Chen**,[2] **and Jianbing Yu**[2]

[1]*School of Transportation, Southeast University, Nanjing, Jiangsu, China*
[2]*College of Civil Science and Engineering, Yangzhou University, Yangzhou, Jiangsu, China*

Correspondence should be addressed to Xuan Guo; guoxuan@yzu.edu.cn

Received 17 July 2018; Accepted 8 October 2018; Published 24 October 2018

Academic Editor: Luigi Di Sarno

Previous earthquake events have shown that chimneys are one of the most fragile structures. Studies have focused on the seismic behavior of reinforced concrete (RC) chimney structures subjected to earthquake load only along the horizontal direction. However, the vertical component of strong ground motion has been proven to damage or completely destroy civil structures. Therefore, it is essential to determine the failure probability of RC chimneys under both horizontal and vertical directions. In this study, the seismic behavior of an RC chimney was studied through seismic fragility analysis, wherein a fragility model based on the intensity ratio between the vertical and horizontal components was proposed. In the fragility analysis, different intensity ratios of near-fault ground motions (NFGMs) between the vertical and horizontal components were considered. The findings indicate that the NFGMs along the vertical and horizontal directions significantly affect the failure probability if the intensity of the horizontal component is above a certain threshold. Moreover, the failure probability increases with the intensity of the vertical and horizontal ground motions. Therefore, the influence of the combination of the vertical and horizontal components of the NFGMs should be considered in the safety evaluation of RC chimney structures.

1. Introduction

Today, with the development in technology and industrial practices, most factories need a chimney structure which is high-rise and slender. Chimney structures can be severely damaged or destroyed during severe wind storms or strong earthquakes. Ghobarah and Baumber [1] pointed out that the fundamental mode of vibration determines the failure of the chimney at its base. In Bońkowski et al. [2], the behavior of an industrial chimney is investigated subjected to translational-horizontal and rocking components of ground motion, and results imply that rotational excitations in the flexural vibrations of the chimney have great influence on the performance of chimney base. In Minghini et al. [3], the risk of a brickwork chimney under 2012 Emilia earthquake is investigated, and the results indicate a shear failure mechanism of the upper part of the chimney. Huang et al. [4] found that the opening and the direction of motion relative to the opening affected the behavior of the chimney. Wilson [5] studied the earthquake responses of ten tall RC chimneys with heights ranging from 115 m to 301 m through nonlinear dynamic analysis. Kilic and Sozen [6] studied the effect of Marmara earthquake (Aug. 17, 1999) on the seismic performance of two RC chimneys with heights of 115 m and 107.5 m. In the Marmara earthquake event, the chimney with a height of 115 m failed. They showed that the presence of reinforcing bar splices caused the failure of the chimney structure. Turkeli et al. [7] studied the response of RC chimneys under wind and earthquake loads and showed that the opening at the body of the chimney can cause brittle failure. Zhou et al. [8] evaluated the damage probability of a high-rise RC chimney with a height of 240 m under seismic loads through seismic fragility analysis (SFA), and some meaningful conclusions were obtained in their study. However, the influence of the vertical component of the ground motions was not considered. Pallares et al. [9] evaluated the capacity of masonry chimneys, which were originally designed to withstand only their weights and wind loads. The structures located in seismic active zones can be potentially subjected to earthquake loads. Through an

experimental study, they pointed out that carbon-fiber-reinforced polymer arranged in the form of vertical strips could protect the chimney structures. Abovementioned studies show that most researchers focused on the performance of chimney structures under horizontal components of ground motions. However, strong earthquake ground motions along the vertical direction have been observed in previous earthquake events, causing severe damage or in some cases complete destruction of bridge structures, building structures, and civil infrastructure facilities [10–13].

Many studies have evaluated the seismic performance of civil structures, such as buildings and bridges, subjected to seismic loads along the vertical direction [14–18]. In Wang et al. [17], they showed that although the effects of the vertical component on the failure probability of piles and expansion bearings were insignificant, the effect on the fixed bearings was significant. They pointed out that the failure probability of certain components of a bridge system can be underestimated if the influence of the vertical ground motion is not considered. Some efforts have been done to study the performance of masonry chimney under vertical ground motions. In Breccolotti and Materazzi [19], the effect of vertical ground motion on the seismic behavior of masonry chimneys was studied; they suggested that the vertical ground motions should not be ignored, particularly in near-fault zones.

The literature review shows that vertical ground motions have great influence on the performance of building, bridge, or other civil structures. Even though some efforts have been done to study the behavior of masonry chimney under horizontal and vertical ground motions, the height and the material properties of masonry chimney are different from that of RC chimneys. Therefore, it is meaningful to study the behavior of RC chimneys under both vertical and horizontal directions simultaneously. In this study, an RC chimney model with a height of 120 m was used to investigate the combined effect of the vertical and horizontal components on the performance through SFA. In the SFA, different intensity ratios between the vertical and horizontal ground motions were considered, and the uncertainty in the NFGMs was also considered. Subsequently, seismic fragility curves and surfaces for different damage states were generated based on the numerical simulation data; the probability of failure depends on the seismic intensity of NFGMs along the horizontal direction and the intensity ratio between the vertical and horizontal components.

2. Seismic Fragility Analysis (SFA)

The seismic fragility assessment is widely employed to determine the probability of damage or of collapse of buildings [20], bridges [21–23], and dams [24], or of other civil structures subjected to earthquake loads. The fragility function equation can be written as follows:

$$P(C < D)|\mathrm{PGA} = \Phi\left(\frac{\ln x - \ln \sigma}{\xi}\right), \tag{1}$$

where $P(C < D)|\mathrm{PGA}$ is the probability of damage or of collapse; C is the structural capacity; D is the seismic demand for a given seismic intensity; PGA denotes the peak ground acceleration; Φ denotes the cumulative normal distribution function; and σ and ξ represent the mean and standard deviation of the seismic intensity that would lead to a damage state, respectively.

For a structure subjected to ground motions along multiple directions (i.e., vertical and horizontal) simultaneously, the fragility function is given as follows:

$$P(C < D)\left|\left(\mathrm{HPGa}, \frac{\mathrm{VPGa}}{\mathrm{HPGa}}\right)\right. = \Phi\left(\frac{\ln x - \ln \sigma_v}{\xi_v}\right), \tag{2}$$

where $P(C < D)|(\mathrm{HPGa}, \mathrm{VPGa/HPGa})$ represents the probability of failure corresponding to a damage state defined under a given horizontal ground motion acceleration intensity (HPGa) and a given ratio between the vertical and horizontal components of the ground motion acceleration intensity (VPGa/HPGa); VPGa denotes the vertical ground motion intensity; and σ_v and ξ_v are the mean and standard deviation of the seismic intensity that leads to a damage state under a given ratio between the vertical and horizontal intensities, respectively. Both σ_v and ξ_v change with respect to the ratio between the vertical and horizontal components of the ground motion intensity. By employing the concept of time-dependent fragility model [25], a VPGa/HPGa-intensity ratio-dependent fragility model was employed in this study; this model can be used to determine the failure probability of structures under different combinations of the vertical and horizontal components of ground motion. The VPGa/HPGa-ratio-dependent fragility function model can be expressed as follows:

$$\sigma_v = p_1\left(\frac{\mathrm{VPGa}}{\mathrm{HPGa}}\right)^2 + p_2\frac{\mathrm{VPGa}}{\mathrm{HPGa}} + p_3, \tag{3}$$

$$\xi_v = p_4\left(\frac{\mathrm{VPGa}}{\mathrm{HPGa}}\right)^2 + p_5\frac{\mathrm{VPGa}}{\mathrm{HPGa}} + p_6, \tag{4}$$

where p_1, p_2, and $p_3$are the estimation parameters for σ_v, whereas p_4, p_5, and p_6 are the estimation parameters for ξ_v.

The probability of exceeding a damage state for any given intensity ratio of ground motion along the two directions (vertical and horizontal) and for a given horizontal ground motion intensity can be computed using Equation (5), as follows:

$$P(C < D)\left|\left(\mathrm{HPGa}, \frac{\mathrm{VPGa}}{\mathrm{HPGa}}\right)\right. = \Phi\left(\frac{\ln x - \ln\left(p_1(\mathrm{VPGa/HPGa})^2 + p_2(\mathrm{VPGa/HPGa}) + p_3\right)}{p_4(\mathrm{VPGa/HPGa})^2 + p_5(\mathrm{VPGa/HPGa}) + p_6}\right). \tag{5}$$

With Equations (3)–(5), the seismic fragility curves and surfaces for different damage states defined in this work can be generated based on the numerical simulation data. The probability of failure at each defined damage state depends on the VPGa/HPGa ratio and the intensity of the horizontal component. The next section presents the NFGMs used in this research for nonlinear dynamic analysis.

3. Near-Fault Ground Motions (NFGMs)

NFGMs recorded within 20 km from the rupture can more severely damage civil structures because of their strong velocity pulse, in comparison with ground motions recorded in the far-field. Bertero et al. [26] investigated the seismic behavior of fixed-base buildings subjected to NFGMs and showed that the NFGMs significantly affect the response of the studied structures. Hall et al. [27] showed that the NFGMs that severely damaged high-rise buildings for the generated demands considerably exceeded the capacity of the structures. In this work, NFGMs were used to investigate their effect on the performance of a chimney structure; the vertical components of the ground motions were included. Many NFGMs can be obtained in PEER ground motion database; thirty of them were downloaded randomly and used in this work for the seismic fragility analysis [28]. These ground motions are mainly recorded from the earthquake events: Chi-Chi Taiwan, Kocaeli Turkey, Darfield New Zealand, and so on. For future study, researchers can use more ground motions. The magnitudes of all the earthquake events used in this research range from 7.0 to 7.62, and the rupture distances of the recorded ground motions are lower than 15 km.

Figure 1(a) shows the time history of the vertical component of the ground motion acceleration with the recorded sequence 1519 corresponding to the Chi-Chi earthquake of Taiwan. Figure 1(b) shows the time history of the velocity, wherein a strong velocity pulse is observed. The design codes suggest that the peak vertical ground motion acceleration ranges from half to three quarters of the horizontal component when the effect of the vertical acceleration need to be considered. However, strong motion recorders from recent earthquake events reveal that the peak ground acceleration of the vertical acceleration may be even higher than that of the horizontal ground motion [14]. The ratio of the vertical peak ground acceleration to the horizontal peak ground acceleration recorded in the near-fault zone is greater than that recorded in the far-field [29, 30]. Therefore, in this study, different intensity ratios are considered, such as 2/3, 4/3, and 6/3.

4. Chimney Model

In this work, an RC chimney with a height of 120 m was used for the SFA. The outside radius of the bottom of the chimney is 6.195 m and that of the top of the chimney is 3.895 m. Figure 2 shows the elevation view of the chimney system. The finite element model of the chimney structure was created by using OpenSees software [31]. The nonlinear beam column element is assigned for the investigated chimney structure. The element size was set as 5.0 m. Mander's model was used to represent the stress-strain relationship of concrete [32]. The concrete compressive strength is 31.0 MPa. Steel02 was employed as the material for the vertical reinforced bars [33]; the steel strength is 336 MPa. It is worth mentioning that the opening on the chimney body was not considered, and the soil structure interaction was not included in this work, as this was not in line with the main objective of this study.

With the created finite element model, nonlinear dynamic analysis was conducted through OpenSees. In this work, the curvature at each section was extracted using the nonlinear dynamic analysis. The curvature was transferred to the curvature ductility demand μ_c, which was employed to judge whether the chimney is damaged. A moment-curvature analysis was performed on each section of the chimney, and the corresponding damage state was defined as follows: slight damage $1 \le \mu_c \le 8.25$, moderate damage $8.25 \le \mu_c \le 13.85$, major damage $13.85 \le \mu_c \le 23.05$, and collapse $\mu_c \ge 23.05$. In the next section, the seismic fragility curve and fragility surface based on the numerical simulation results are introduced.

5. Fragility Curves and Surfaces Based on Numerical Simulation Results

5.1. Fragility Curves of the Chimney under the Combined Effect of Vertical and Horizontal Components of NFGMs. With the chimney model presented in Section 4 and the NFGMs given in Section 3, a nonlinear dynamic analysis was performed. Based on the numerical simulation data, fragility curves were generated using Equation (2) by following the procedure provided by Baker [34]. Figure 3(a) shows the probability of slight damage. Figure 3(b) presents the probability of moderate damage. Figures 3(c) and 3(d) show the probability of major damage and collapse, respectively.

Figure 3(b) clearly shows that the combined influence of the vertical and horizontal components of the NFGMs significantly influences the probability of moderate damage when the intensity of the horizontal component is greater than 0.5 g. The probability of moderate damage increases with the intensity ratio. Figure 3(d) shows that the collapse probability of the studied chimney structure increases with the intensity ratio VPGa/HPGa when the intensity of the horizontal component is greater than 1.0 g. When the horizontal ground motion intensity is 1.5 g with an intensity ratio of 2.0, the probability of collapse of the chimney structure is approximately 12%, which is approximately twice that under the horizontal component alone with an intensity of 1.5 g. Therefore, the influence of the near-fault vertical component of the earthquake ground motions on the safety of RC chimney structures should not be neglected.

5.2. Fragility Surfaces of the Chimney Subjected to NFGMs along Both Vertical and Horizontal Directions. In Section 5.1, the fragility curves are generated through numerical simulation data for different damage states with different intensity ratios. Based on Equations (3) and (4), the models of σ_v and ξ_v can be obtained using the least square fitting method. With Equation (5), the seismic fragility surface corresponding to each damage state of the chimney structure subjected to NFGMs including their vertical components can be generated efficiently. The probability of exceeding a damage state at any intensity combination of vertical and

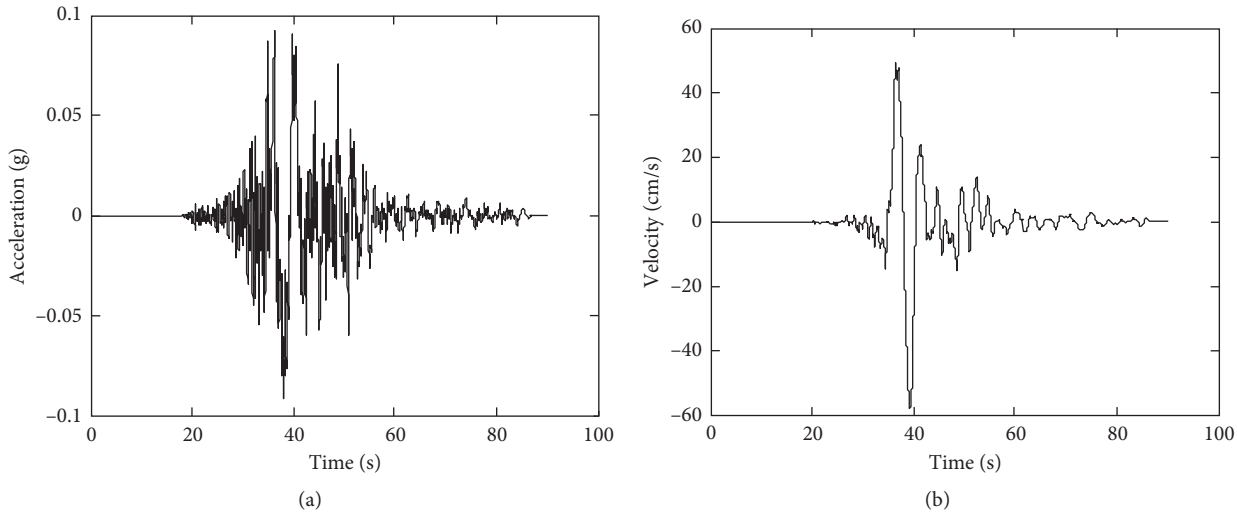

Figure 1: Time history of RSN1519 Chi-Chi Taiwan: (a) acceleration; (b) velocity.

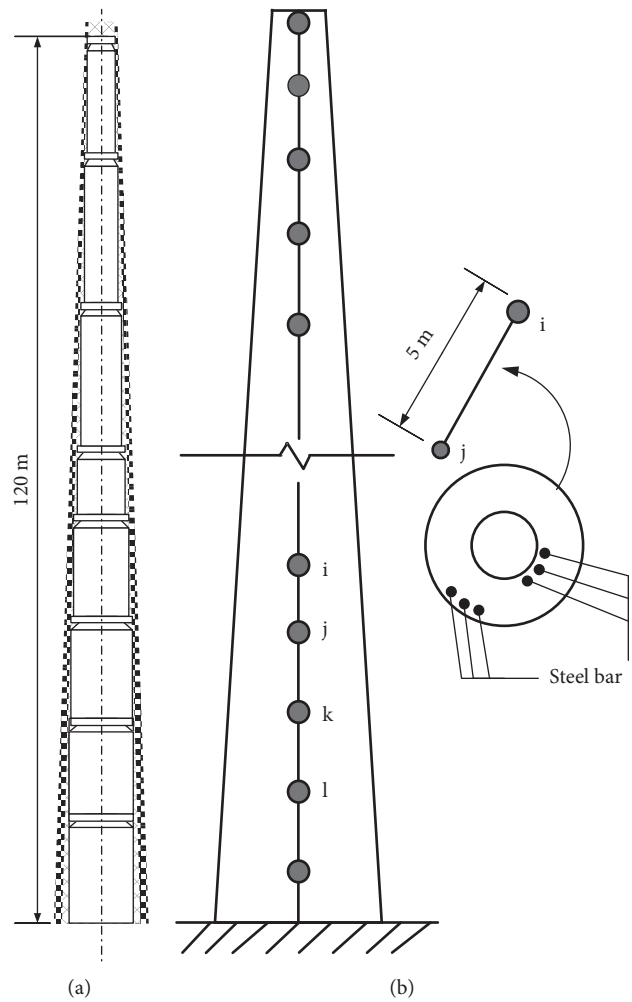

Figure 2: Elevation view of the chimney model: (a) geometry model; (b) finite element model.

horizontal components of the earthquake ground motion can be computed effectively without performing nonlinear dynamic analysis again.

Figures 4(a) and 4(b) show the seismic fragility surface for exceeding the slight damage state and moderated damage state, respectively. Figures 4(c) and 4(d) present

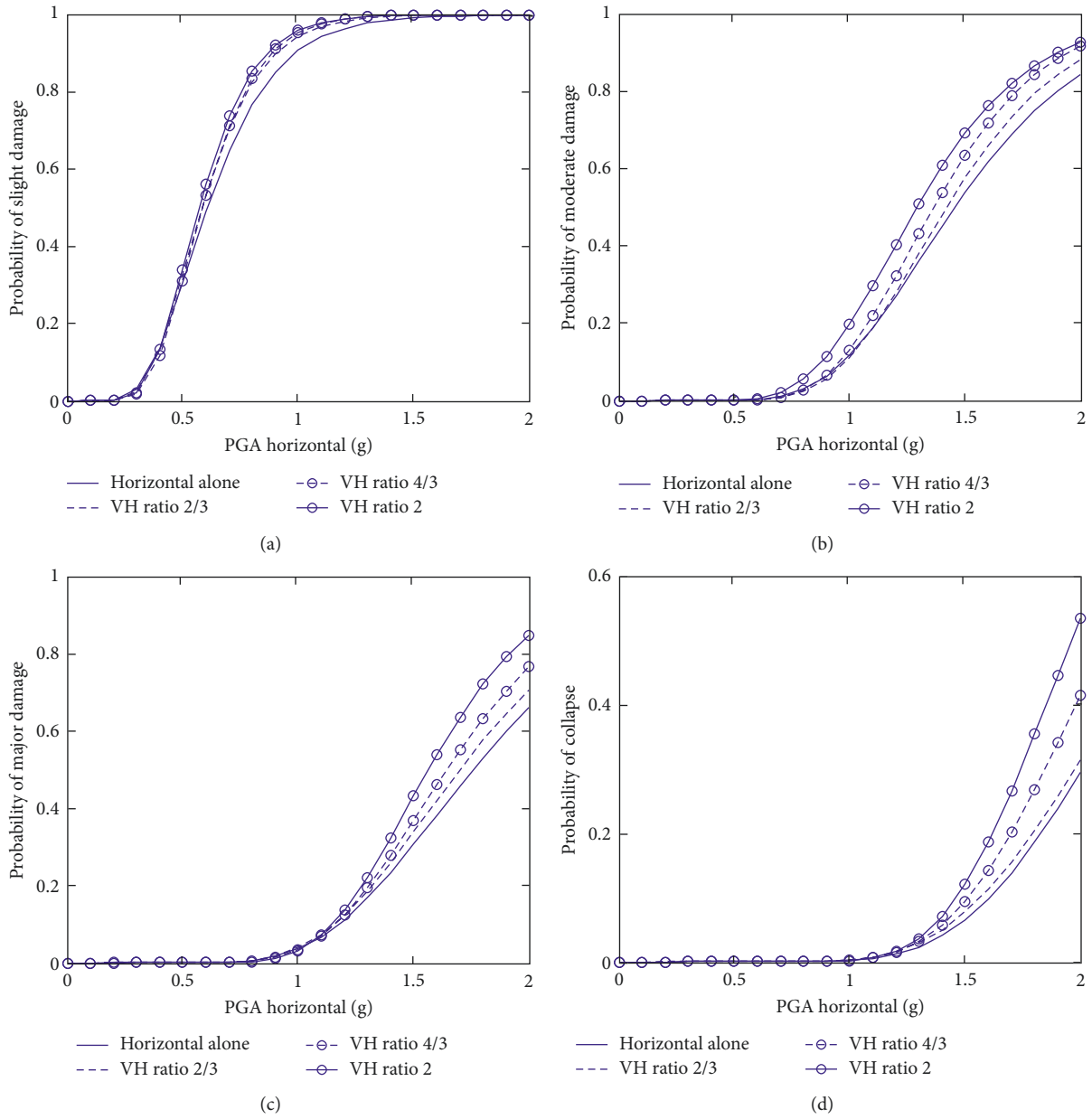

Figure 3: Fragility curves of the chimney structure for different damage states: (a) slight; (b) moderate; (c) major; and (d) collapse.

the probability of major damage and collapse. From Figure 4, it is clear that the vertical ground motions significantly affect the probability of moderate damage when the intensity of the horizontal ground motion is greater than 0.5 g. Moreover, the motions significantly affect the probability of major damage when the intensity of the horizontal ground motion is greater than 0.8 g. They significantly affect the probability of collapse when the horizontal component intensity of the ground motions is greater than 1.0 g. Therefore, it can be concluded that the effect of the NFGMs along the vertical direction on the probability of exceeding a damage state depends on the intensity level of the horizontal component of the ground motions.

6. Discussion and Conclusions

6.1. Discussion. In this work, a chimney model was employed for the SFA based on the vertical ground motion. The chimney structure was subjected to NFGMs along both the vertical and horizontal directions. The findings of this work show that the probability of slight damage is significantly affected by the intensity ratio, as it increases dramatically when the intensity of the ground motions along the horizontal direction is over 0.4 g and when it is lower than 1.0 g. However, the effect of the intensity ratio on the probability of slight damage is less if the intensity of the ground motions along the horizontal direction is higher than 1.0 g, as the seismic fragility curves increase slowly, and the

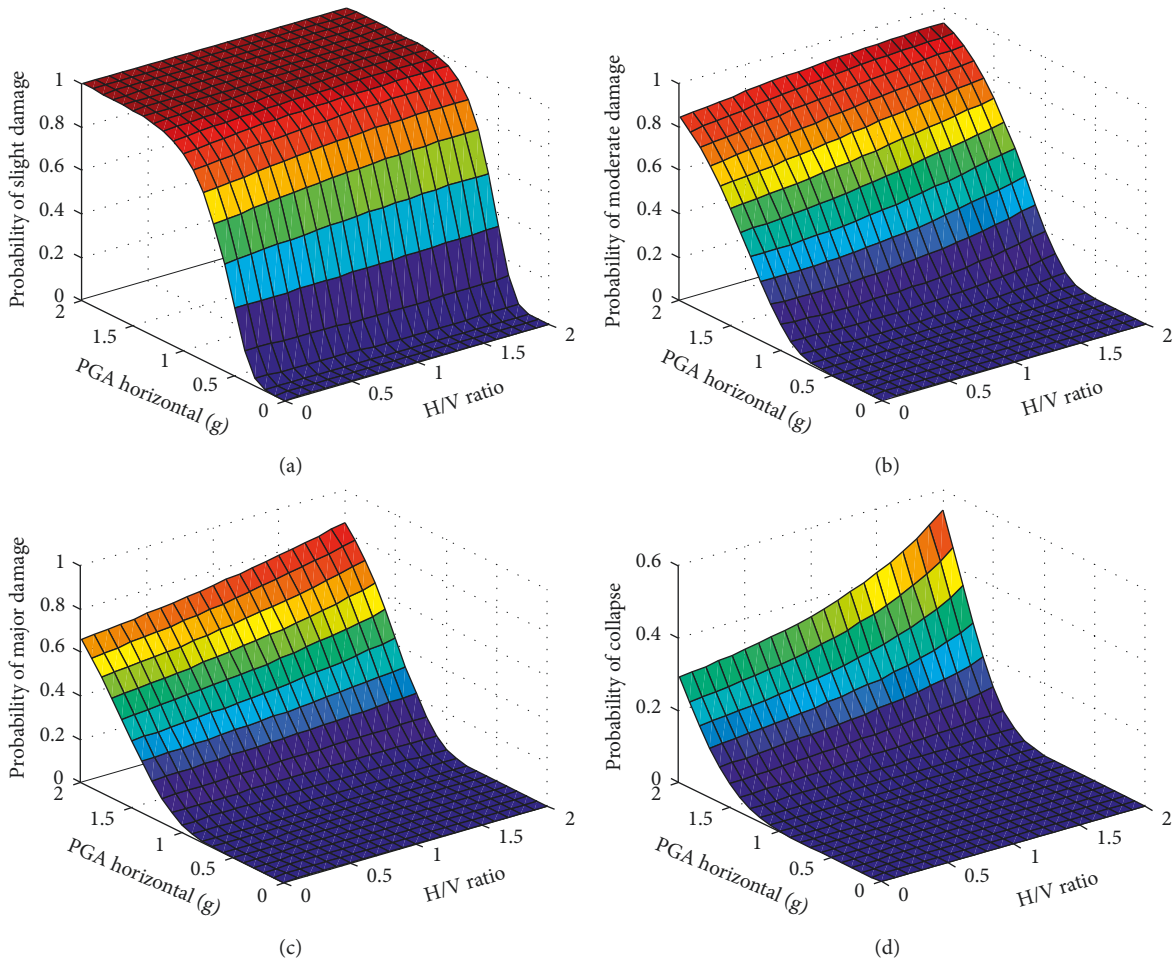

Figure 4: Fragility surfaces for different damage states: (a) slight; (b) moderate; (c) major; and (d) collapse.

probabilities of slight damage for all intensity ratios are largely the same. Thus, the intensity ratio has less impact on the slight damage state when the intensity of the horizontal component is very high. For the probability of moderate damage, the probabilities increase sharply for all the intensity ratios if the intensity of the horizontal component is higher than 0.6 g. For the major damage state, the probabilities increase dramatically for all the intensity ratios if the intensity of the horizontal component is greater than 1.0 g. The overall trends of the moderate and major damage states are largely the same. The probability of collapse increases slowly when the intensity of the horizontal component is lower than 1.2 g. However, it decreases dramatically when the horizontal component intensity is higher than 1.2 g.

The results of this study show that the probabilities of each of the defined damage states nonlinearly increase with respect to the intensity ratio and horizontal component intensity. Moreover, the nonlinearity depends on the degree of the damage defined in this research. The effects of the intensity ratio and the horizontal component intensity on the damage probability are less when they are lower than a specific threshold. The damage probability increases dramatically with VPGa/HPGa and horizontal component intensity when they are higher than the threshold. The threshold values of VPGa/HPGa and the horizontal component intensity increase if the damage state is changed from slight damage to collapse. For example, if the intensity of the horizontal ground motion is lower than 1.0 g, the collapse probability is close to 0. The changes in the horizontal and vertical intensities of the NFGMs significantly affect the collapse probability when the intensity of the horizontal component is greater than 1.0 g.

Although the study considers an RC chimney model commonly used in industries and provides some meaningful findings, the results may not be applicable to other geometric configurations and other types of chimney structures. Further analysis is required to study the combined influence of the vertical and horizontal intensities of NFGMs on the probability of failure of more soil-foundation-chimney structure systems. The effect of NFGMs along the vertical direction on the behaviors of other types of chimney structures (steel chimney and masonry chimney) should be studied. In order to reduce computation cost, a two-dimensional model was created for the chimney structure as done in Zhou et al. [8] in this work. In future research, it is suggested to create a three-dimensional model to simulate chimney structure to enhance the accuracy of calculation results.

7. Conclusions

In this work, the combined influence of the vertical and horizontal components of NFGMs on the failure probability of an RC chimney structure was investigated through SFA. A seismic fragility function model based on the ratio between the vertical and horizontal intensities was proposed. In the fragility analysis, the uncertainty in the NFGMs was considered. Fragility curves and surfaces with different damage states were generated based on the nonlinear dynamic analysis results. The failure probability of different damage states was found to depend on the intensity ratio and the horizontal component intensity. The findings show that the combined influence of the vertical and horizontal components of NFGMs significantly affect the damage states defined in this research if the intensity of the horizontal component of the ground motions is greater than a threshold value. Therefore, this combined effect should be considered in the safety evaluation of chimney structures located close to near-fault zones.

Data Availability

The data used to support the findings of this study are included within the article.

Conflicts of Interest

The authors declare that they have no conflicts of interest.

Acknowledgments

The authors thank the support from the NSFC (Grant No. 51708484), NSFJP (Grant No. BK20170511), the Natural Science Foundation of the Jiangsu Higher Education Institutions of China (Grant No. 17KJB580010), and the China Postdoctoral Science Foundation (Grant No. 2017M611658).

References

[1] A. Ghobarah and T. Baumber, "Seismic response and retrofit of industrial brick masonry chimneys," *Canadian Journal of Civil Engineering*, vol. 19, no. 1, pp. 117–128, 2011.

[2] P. A. Bońkowski, Z. Zembaty, and M. Yan Minch, "Time history response analysis of a slender tower under translational-rocking seismic excitations," *Engineering Structures*, vol. 155, pp. 387–393, 2018.

[3] F. Minghini, G. Milani, and A. Tralli, "Seismic risk assessment of a 50m high masonry chimney using advanced analysis techniques," *Engineering Structures*, vol. 69, no. 9, pp. 255–270, 2014.

[4] W. Huang, P. L. Gould, R. Martinez, and G. S. Johnson, "Non—linear analysis of a collapsed reinforced concrete chimney," *Earthquake Engineering & Structural Dynamics*, vol. 33, no. 4, pp. 485–498, 2010.

[5] J. L. Wilson, "Earthquake response of tall reinforced concrete chimneys," *Engineering Structures*, vol. 25, no. 1, pp. 11–24, 2003.

[6] S. A. Kilic and M. A. Sozen, "Evaluation of effect of august 17, 1999, Marmara earthquake on two tall reinforced concrete chimneys," *ACI Structural Journal*, vol. 100, no. 3, pp. 357–364, 2003.

[7] E. Turkeli, Z. Karaca, and H. T. Ozturk, "On the wind and earthquake response of reinforced concrete chimneys," *Earthquakes and Structures*, vol. 12, no. 5, pp. 559–567, 2017.

[8] C. Zhou, X. Zeng, Q. Pan, and B. Liu, "Seismic fragility assessment of a tall reinforced concrete chimney," *Structural Design of Tall a Special Buildings*, vol. 24, no. 6, pp. 440–460, 2015.

[9] F. J. Pallares, S. Ivorra, L. Pallares, and J. M. Adam, "Seismic assessment of a CFRP-strengthened masonry chimney," *Proceedings of the Institution of Civil Engineers-Structures and Buildings*, vol. 162, no. 5, pp. 291–299, 2009.

[10] E. Watanabe, K. Sugiura, K. Nagata, and Y. Kitane, "Performances and damages to steel structures during 1995 Hyogoken-Nanbu earthquake," *Engineering Structures*, vol. 20, no. 4–6, pp. 282–290, 1998.

[11] F. Naeim, M. Lew, S. C. Huang, H. K. Lam, and L. D. Carpenter, "The performance of tall buildings during the 21 September 1999 Chi–Chi earthquake Taiwan," *The Structural Design of Tall Buildings*, vol. 9, no. 2, pp. 137–160, 2000.

[12] Federal Emergency Management Agency, "State of art report on past performance of steel moment frame buildings in earthquakes," Rep. No. FEMA 355E, Washington, DC, USA, 2000.

[13] A. J. Papazoglou and A. S. Elnashai, "Analytical and field evidence of the damaging effect of vertical earthquake ground motion," *Earthquake Engineering and Structural Dynamics*, vol. 25, no. 10, pp. 1109–1137, 1996.

[14] A. Ghobarah and A. S. Elnashai, "Contribution of Vertical ground motion to the damage of RC buildings," in *Proceedings of European Conference on Earthquake Engineering*, Paris, France, September 1998.

[15] Y. Xiang, Y. F. Luo, Z. C. Zhu, and Z. Y. Shen, "Estimating the response of steel structures subjected to vertical seismic excitation: idealized model and inelastic displacement ratio," *Engineering Structures*, vol. 148, pp. 225–238, 2017.

[16] L. D. Sarno, A. S. Elnashai, and G. Manfredi, "Assessment of RC columns subjected to horizontal and vertical ground motions recorded during the 2009 L'Aquila (Italy) earthquake," *Engineering Structures*, vol. 33, no. 5, pp. 1514–1535, 2011.

[17] Z. Wang, J. E. Padgett, and L. Dueñas-Osorio, "Influence of vertical ground motions on the seismic fragility modeling of a bridge-soil-foundation system," *Earthquake Spectra*, vol. 29, no. 3, pp. 937–962, 2013.

[18] M. R. Button, R. L. Mayes, and C. J. Cronin, "Effect of vertical motions on seismic response of highway bridges," *Journal of Structural Engineering*, vol. 128, no. 12, pp. 1551–1564, 2002.

[19] M. Breccolotti and A. L. Materazzi, "The role of the vertical acceleration component in the seismic response of masonry chimneys," *Materials and Structures*, vol. 49, no. 1-2, pp. 29–44, 2016.

[20] M. S. Kirçil and Z. Polat, "Fragility analysis of mid-rise R/C frame buildings," *Engineering Structures*, vol. 28, no. 9, pp. 1335–1345, 2006.

[21] M. Shinozuka, M. Q. Feng, J. Lee, and T. Naganuma, "Statistical analysis of fragility curves," *Journal of Engineering Mechanics*, vol. 126, no. 12, pp. 1224–1231, 2000.

[22] Y. Pan, A. K. Agrawal, M. Ghosn, and S. Alampalli, "Seismic fragility of multispan simply supported steel highway bridges in New York State. II: fragility analysis, fragility curves, and fragility surfaces," *Journal of Bridge Engineering*, vol. 15, no. 5, pp. 462–472, 2010.

[23] X. Guo, Y. Wu, and Y. Guo, "Time-dependent seismic fragility analysis of bridge systems under scour hazard and earthquake loads," *Engineering Structures*, vol. 121, pp. 52–60, 2016.
[24] B. Ellingwood and P. B. Tekie, "Fragility analysis of concrete gravity dams," *Journal of Infrastructure Systems*, vol. 7, no. 2, pp. 41–48, 2001.
[25] J. Ghosh and J. E. Padgett, "Aging considerations in the development of time-dependent seismic fragility curves," *Journal of Structural Engineering*, vol. 136, no. 12, pp. 1497–1511, 2010.
[26] V. V. Bertero, S. A. Mahin, and R. A. Herrera, "A seismic design implications of near-fault San Fernando earthquake records," *Earthquake engineering Structural Dynamics*, vol. 6, no. 1, pp. 31–42, 1978.
[27] J. F. Hall, T. H. Heaton, M. W. Halling, and D. J. Wald, "Near-source ground motion and its effects on the flexible buildings," *Earthquake spectra*, vol. 11, no. 4, pp. 569–605, 1995.
[28] PEER, *PEER Ground Motion Database*, 2015, http://peer.berkely.edu/2015.
[29] Y. Bozorgnia and K. W. Campbell, "The vertical-to-horizontal response spectral ratio and tentative procedures for developing simplified V/H and vertical design spectra," *Journal of Earthquake Engineering*, vol. 8, no. 2, pp. 175–207, 2004.
[30] A. Elgamal and L. He, "Vertical earthquake ground motion records: an overview," *Journal of Earthquake Engineering*, vol. 8, no. 5, pp. 663–697, 2004.
[31] OpenSees, *The Open System for Earthquake Engineering Simulation*, 2014, http://opensees.berkeley.edu/2014/05.
[32] J. B. Mander, M. J. Priestley, and R. Park, "Theoretical stress-strain model for confined concrete," *Journal of Structural Engineering*, vol. 114, no. 8, pp. 1804–1826, 1998.
[33] S. Mazzoni, F. McKenna, M. H. Scott, and G. L. Fenves, *OpenSees Command Language Manual*, Pacific Earthquake Engineering Research (PEER) Center, Berkeley, CA, USA, 2006.
[34] J. W. Baker, "Efficient analytical fragility function fitting using dynamic structural analysis," *Earthquake Spectra*, vol. 31, no. 1, pp. 579–599, 2015.